Journal of Colloid and Interface Science 653 (2024) 1283–1292

Contents lists available at ScienceDirect

Journal of Colloid And Interface Science

journal homepage: www.elsevier.com/locate/jcis

Unraveling the role of polysaccharide-goethite associations on glyphosate' adsorption–desorption dynamics and binding mechanisms

Behrooz Azimzadeh, Carmen Enid Martínez *

Soil and Crop Sciences, School of Integrative Plant Science, College of Agriculture and Life Sciences, Cornell University, Ithaca, NY 14853, USA

GRAPHICAL ABSTRACT

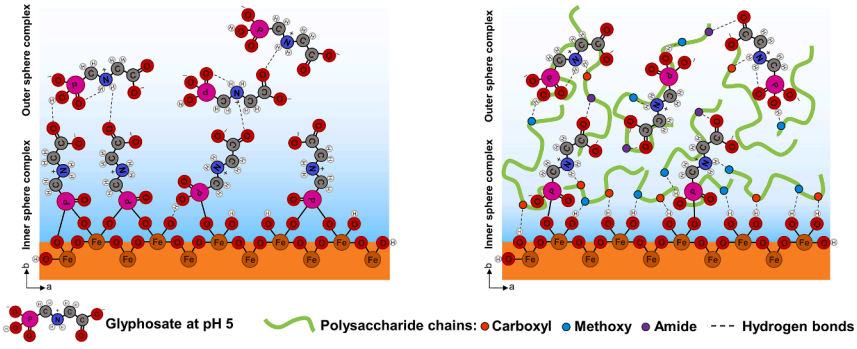

ARTICLE INFO

Keywords:
Organo-mineral associations
Organic-organic interactions
Polysaccharide-goethite complex
Adsorption
Desorption
Kinetics
In-situ ATR-FTIR
XPS
Inner- and outer-sphere complexes
Noncovalent interactions

ABSTRACT

Hypothesis: Glyphosate retention at environmental interfaces is strongly governed by adsorption and desorption processes. In particular, glyphosate can react with organo-mineral associations (OMAs) in soils, sediments, and aquatic environments. We hypothesize mineral-adsorbed biomacromolecules modulate the extent and rate of glyphosate adsorption and desorption where electrostatic and noncovalent interactions with organo-mineral surfaces are favored.

Experiments: Here we use *in-situ* attenuated total reflectance Fourier-transform infrared, X-ray photoelectron spectroscopy, and batch experiments to characterize glyphosate' adsorption and desorption mechanisms and kinetics at an organo-mineral interface. Model polysaccharide-goethite OMAs are prepared with a range of organic (polysaccharide, PS) surface loadings. Sequential adsorption–desorption studies are conducted by introducing glyphosate and background electrolyte solutions, respectively, to PS-goethite OMAs.

Findings: We find the extent of glyphosate adsorption at PS-goethite interfaces was reduced compared to that at the goethite interface. However, increased polysaccharide surface loading resulted in lower relative glyphosate desorption. At the same time, increased PS surface loading yielded slower glyphosate adsorption and desorption kinetics compared to corresponding processes at the goethite interface. We highlight that adsorbed PS promotes the formation of weak noncovalent interactions between glyphosate and PS-goethite OMAs, including the evolution of hydrogen bonds between (*i*) the amino group of glyphosate and PS and (*ii*) the phosphonate group of

* Corresponding author.
E-mail address: cem20@cornell.edu (C.E. Martínez).

https://doi.org/10.1016/j.jcis.2023.09.141
Received 6 June 2023; Received in revised form 29 August 2023; Accepted 23 September 2023
Available online 26 September 2023

glyphosate and goethite. It is also observed that glyphosate' phosphonate group preferentially forms inner-sphere monodentate complexes with goethite in PS-goethite whereas bidentate configurations are favored on goethite.

1. Introduction

Glyphosate (*N*-(phosphonomethyl)glycine) is applied to agricultural crops, side roads, and individuals' home gardens and lawns. Upon application, glyphosate interacts with mineral and organic-coated mineral surfaces potentially affecting its mobility and efficacy as an herbicide. Since the mobility and distribution of herbicides in soil is generally mediated by water transport, adsorption–desorption processes at these interfaces are deemed important. Glyphosate is the world's most heavily applied herbicide [1] and its widespread use has raised concerns about its effects on human health and the environment [2–4]. Glyphosate is a polar organic molecule and a zwitterion at relevant environmental conditions, with a tridentate character due to its amino, carboxylic, and phosphonic functional groups [5,6]. A large number of studies show that glyphosate can strongly interact with metal ions in solution and at water–mineral interfaces [4,5,7–10], particularly with iron (hydr)oxides through its phosphonic group [7–9,11–15].

The role of organic-coated mineral surfaces (i.e., organo-mineral associations, OMAs) on the retention, mobility and distribution of glyphosate in soils is far less studied and understood. A few studies have shown that OMAs may inhibit, hinder or enhance the mobility of glyphosate in the environment [12,16]. For example, humic acid-goethite associations have been shown to increase glyphosate mobility, presumably a result of electrostatic repulsion due to the negative charge conferred by sorbed humic acid and by a reduction in the availability of active mineral surface sites [12]. Conversely, a more recent study [16] demonstrated that a humic acid-kaolinite association can adsorb higher amounts of glyphosate than kaolinite alone. In the latter study, the authors suggest a ternary adsorption system in which glyphosate binds to the interfacial hydroxyl groups in humic acid-kaolinite associations via hydrogen bonds involving carboxyl, amino, and phosphonyl functional groups of glyphosate. Based on these disparate results, we are unable to conceptualize or predict the effect OMAs might have on glyphosate retention. Besides, previous studies have failed to consider desorption dynamics when assessing glyphosate behavior at these heterogeneous organo-mineral interfaces and have used humic acids as model organic coatings. Humic acids (together with fulvic acids) are an operationally defined organic fraction extracted from soils and do not represent the biomolecules present in soils [17].

To address this void in knowledge, we present a series of molecular-scale, time-resolved, and surface-sensitive adsorption–desorption studies using goethite and polysaccharide-goethite associations as model interfaces. A clear understanding of the molecular structure of an OMA is essential to accurately probe glyphosate behavior and fate. We used goethite (α-FeOOH) as the model mineral in experiments because it is commonly present in soils and frequently used in glyphosate sorption studies [9,12,14,18–21].

The adsorption of biomacromolecules onto mineral surfaces may be driven by forces that include H-bonding, ion exchange, ligand exchange, and electrostatic, hydrophobic and van der Waals interactions. Adsorption of these biomacromolecules, for example proteins [22–24], nucleic acids [25–27], lipids [28], polysaccharides [29,30], and extracellular polymeric substances [31–33] onto mineral surfaces not only influences organic and mineral reactivity in environmental systems, but rather, the newly formed organo-mineral interfaces can modulate biogeochemical processes in soils and sediments [34,35]. We chose a polysaccharide (i.e., a naturally occurring biomacromolecule present in plant cell walls and therefore a major component of organic matter in soils) as the model organic molecule present in OMAs. Polysaccharides (PS) are ubiquitous in soils and potentially act as binding agents in the soil matrix [36,37]. Unlike humic and fulvic acids, the structure of the chosen PS (pectin) is well-known: a linear polymer composed of α-1,4-linked galacturonic acid units. The galacturonic acid units could be methoxylated and/or amidated to various degrees [38,39].

In this study, we determine the extent, kinetics and mechanisms of interaction of glyphosate at PS-goethite and goethite interfaces and investigate the effect increasing polysaccharide surface loading might have on these processes. All experiments were conducted at pH = 5.0 to simulate agricultural soils of humid climates where the affinity of glyphosate for soil particles is high and where soils are rich in iron (hydr)oxides and organic matter [40–42]. Experimentally, we use *in-situ* time-resolved attenuated total reflectance Fourier transform infrared (ATR-FTIR) spectroscopy to obtain adsorption–desorption kinetic parameters and to decipher glyphosate' mechanisms of interaction. The capabilities of ATR-FTIR to obtain kinetic information of environmentally relevant systems has been demonstrated in several studies [12,22,43]. Batch and X-ray photoelectron spectroscopy (XPS) experiments are conducted to further characterize the extent of glyphosate adsorption–desorption dynamics at PS-goethite interfaces. The use of XPS to acquire surface coverage and chemical bonding information at glyphosate-mineral and biomolecule-mineral interfaces has been established [9,26,44]. In addition, a homonuclear proton saturation transfer difference nuclear magnetic resonance (STD-NMR) experiment [45] was conducted to learn whether glyphosate and PS molecules interact in solution.

Furthermore, we decipher the contribution of each functional group of glyphosate (amino, carboxylate, phosphonate) to its interaction with goethite and with polysaccharide-goethite associations during adsorption and desorption processes. To the best of our knowledge, this is the first study highlighting glyphosate' adsorption–desorption dynamics at polysaccharide-goethite interfaces at the molecular-scale, in solution and in real time. These studies provide new knowledge that further our understanding of glyphosate' sorption–desorption dynamics at heterogeneous organo-mineral interfaces.

2. Materials and methods

2.1. Materials

Glyphosate (96% purity) was purchased from Sigma-Aldrich (Milwaukee, USA). Amidated high methoxyl pectin was acquired from Sigma-Aldrich. This pectin, a polysaccharide (PS), is used as the model biomacromolecule in our study and it has a *MW* of ≈ 71100 g mol^{-1} [46–48], and a $pK_{a(COOH)}$ = 3.3–4.5 [49]. The galacturonic acid (GalA), methoxy and amide contents were calculated as 37.1, 58.7, 4.2%, respectively (see SM1 in supplementary information (SI) for details). All solutions and suspensions were made with deionized water (18.2 MΩ resistance), boiled and purged with N_2 gas to remove dissolved CO_2. In all experiments, a 10 mM KCl background electrolyte was used to approximate the low ionic strength of soil solutions. Goethite (α-FeOOH) was synthesized by the method of Schwertmann and Cornell [50]. Details of mineral synthesis and characterization can be found in SI (SM2 and Fig. S1). The pH at the point of zero charge (pH_{pzc}) of the synthesized goethite was 8.4 ± 0.2 (Fig. S2 in SI).

2.2. ^1H saturation-transfer difference (STD) NMR experiment

Saturation transfer difference (STD) NMR experiments were used to probe potential interactions between glyphosate and the PS in solution. For the most sensitive STD-NMR spectra, a 20 μM PS solution was prepared in D_2O (99.9 atom% D, Cambridge Isotope Laboratories Inc.). Then, 0.35 mg glyphosate was dissolved in 2 mL of the PS solution

([glyphosate] = 1.0 mM) to yield a 50-fold excess glyphosate to ligand (PS) ratio [51]. The pH was adjusted to 5 using potassium deuteroxide (40 wt% in D_2O, ≥ 99 atom% D, Sigma) and deuterium chloride (35 wt% in D_2O, ≥ 99 atom% D, Sigma). ^{1}H STD-NMR experiments were conducted on a 600 MHz Varian Inova NMR spectrometer at 25 °C. STD parameters were selected based on values reported in a previous study [45]. Spectra were processed in MNova software (v. 14.3, Mestrelab Research S.L.).

2.3. Batch experiments, XPS and zeta potential analyses

Batch adsorption–desorption studies were conducted to quantify glyphosate adsorption and desorption from experimental surfaces, and to obtain qualitative and quantitative information about the surface characteristics and bonding environment of complexes using zeta potential and X-ray photoelectron spectroscopy (XPS) measurements. Procedural details of the batch experiments are described in SI, SM3. Briefly, a series of PS-goethite OMAs were synthesized with varying PS surface loading (i.e., Phases 1 and 2). Then, glyphosate adsorption and desorption experiments were conducted at pH 5 by addition of a 1 mM glyphosate solution to the prepared PS-goethite OMAs (adsorption, Phase 3), followed by desorption (Phase 4) using a 10 mM KCl background solution. The supernatants were filtered (0.2 μm) and analyzed using a TOC-L analyzer (Shimadzu Scientific Instruments) along with standard polysaccharide solutions. Glyphosate concentrations were also measured using a colorimetric approach after derivatization in 2 mM fluorenyl orthochloroformate and 20 mM borate buffer solutions [52,53]. XPS analyses were conducted on selected pellets and required standards. Details of XPS analyses are presented in SI, SM4. For zeta potential measurements, all of the pellets were resuspended in background solution and measured with a Zetasizer (Nano ZS90, Malvern instruments Ltd., UK). BET surface area (N_2 adsorption) and scanning electron microscopy (SEM) images were obtained with an ASAP2460 instrument (Micromeritics Instrument Corp.) and a Zeiss Gemini 500 FE-SEM, respectively.

2.4. In-situ time-resolved ATR-FTIR adsorption-desorption experiments

The workflow of *in-situ* ATR-FTIR (attenuated total reflectance Fourier transform infrared) experiments (Fig. S3) and methodological details are reported in SI (SM5 and SM6). The formation of PS-goethite complexes was initiated by introducing PS solutions over a hydrated layer of goethite on the surface of the ATR crystal. A range of surface loadings were obtained by passing different initial concentrations of PS ([PS] = 0, 4, 8, 14, 28, 42, and 56 μM) over goethite films for a fixed time (coating, Phase 1 ≈ 180 min). Adsorbed PS was stabilized by passing 10 mM KCl background electrolyte to remove any loosely bound PS. Stability of PS-goethite complexes was considered attained when no changes were observed in interfacial spectra collected during background solution flow (stabilization, Phase 2 ≈ 60 min). At this point, a background spectrum was collected, and adsorption of glyphosate was initiated by exchanging the background solution with a fixed 4.0 mM glyphosate solution (adsorption, Phase 3 ≈ 86 min). A glyphosate concentration of 4.0 mM was chosen to minimize instrumental noise and unwanted spectral artifacts on collected interfacial spectra. Glyphosate adsorption was followed by a desorption experiment using the same background solution until equilibrium (desorption, Phase 4 ≈ 72 min). Solutions with a pH of 5.0 were used for all experiments, which model environmentally relevant conditions representative of agricultural soils of humid regions (I = 10 mM and pH = 5.0). The pH was maintained within 0.05 pH units by regulated additions of 0.005 M HCl or KOH with a pH controller. Experiments were repeated 4 times on freshly prepared films under identical conditions. All the *in-situ* experiments were conducted under ambient atmosphere and using a close flow through system at a rate of 0.85 ± 0.05 mL min^{-1} (flow velocity = 4.5 × 10^{-3} m s^{-1}) using a peristaltic pump (Cole-Parmer, IL). Bulk solution spectra of glyphosate and polysaccharide were collected at concentrations of 0.10 M and 112.0 μM, respectively, in a 10 mM KCl background solution at pH = 5.0. All spectra were collected by subtracting the spectrum of the background electrolyte from the spectrum of each sample. In this way, the difference spectrum contains only the absorption bands of interfacial species, including inner- and outer-sphere species and bands of free or uncomplexed species in the bulk solutions.

2.5. ATR-FTIR data processing for analyses

Two regions, the phosphonate frequency region (1100 – 950 cm^{-1}, $\nu(PO)$) and the carboxylate-amine frequency region (1700 – 1500 cm^{-1}, $\nu(CAc)$), were cut and further processed. The integral of the baseline-corrected IR peaks of the phosphonate region was used to probe total glyphosate adsorption and desorption kinetics and P—O band coordination to Fe(III). The spectral features in the 1700 – 1500 cm^{-1} range were deconvoluted in order to determine potential hydrogen bonding and the contribution of carboxylate ($\nu_{as}(COO^-)$) and amine ($\delta(NH_2^+)$) functionalities in interfacial complex formation and subsequent dynamicity of adsorbed glyphosate. Deconvolution of the $\nu(CAc)$ band at the goethite and PS-goethite interfaces is fully explained in SI, SM7. Peak fitting of the spectra was carried out using a second derivative deconvolution algorithm using PeakFit package v.4.12 (Systat Software Inc., San Jose, CA).

2.6. Glyphosate adsorption-desorption kinetic models

Integral of FTIR bands ($A(\tilde{\nu}_i)$) of glyphosate moieties during adsorption and desorption experiments were fitted with two commonly used kinetic models, the Lagergren's pseudo-second-order (PSO) and pseudo-first-order (PFO) models, respectively [54,55]. The PSO model for adsorption processes can be described by the following equation [56]:

$$A(\widetilde{\nu}_i)_{t,ads} = \frac{k_{2,ads}A(\widetilde{\nu}_i)^2_{e,ads}t}{1 + k_{2,ads}A(\widetilde{\nu}_i)_{e,ads}t} \quad (1)$$

where $A(\tilde{\nu}_i)_{t,ads}$ is the integral absorption intensity of the glyphosate band (a.u.) at adsorption time t (min), $k_{2,ads}$ is the PSO rate constant (min^{-1} a.u.$^{-1}$), and $A(\tilde{\nu}_i)_{e,ads}$ is the integral absorption intensity of the glyphosate band at equilibrium (a.u.).

Desorption of glyphosate was described by a modified PFO model represented by the following equation [43]:

$$A\left(\widetilde{\nu}_i\right)_{t,des} = \left(\alpha - A\left(\widetilde{\nu}_i\right)_{e,des}\right)e^{-k_{1,des}t} + \alpha \quad (2)$$

where $A(\tilde{\nu}_i)_{t,des}$ is the integral absorption intensity of the glyphosate band (a.u.) at desorption time t (min), $k_{1,des}$ is the PFO rate constant (min^{-1}), $A(\tilde{\nu}_i)_{e,des}$ is the integral absorption intensity of the glyphosate band at the end of the desorption phase (a.u.), and α is a dimensionless constant that locates the desorption curve that follows just after the adsorption curve at equilibrium. The PFO model was also applied to describe PS's adsorption and desorption kinetics at the goethite interface during formation and stabilization of PS-goethite OMAs (see SI, SM8 for details). All fitting was completed with the nonlinear curve fitting GraphPad Prism v.9.0 software (GraphPad Inc, San Diego, CA).

3. Results and discussion

3.1. Glyphosate attaches to polysaccharide chains

The ^{1}H STD-NMR spectra of glyphosate with and without PS are shown in Fig. 1. The singlet peak (H1) corresponds to protons next to the glyphosate carboxyl group, while the doublet (H2) derives from proton splitting due to geminal coupling with the P nucleus [45,57]. Weak STD

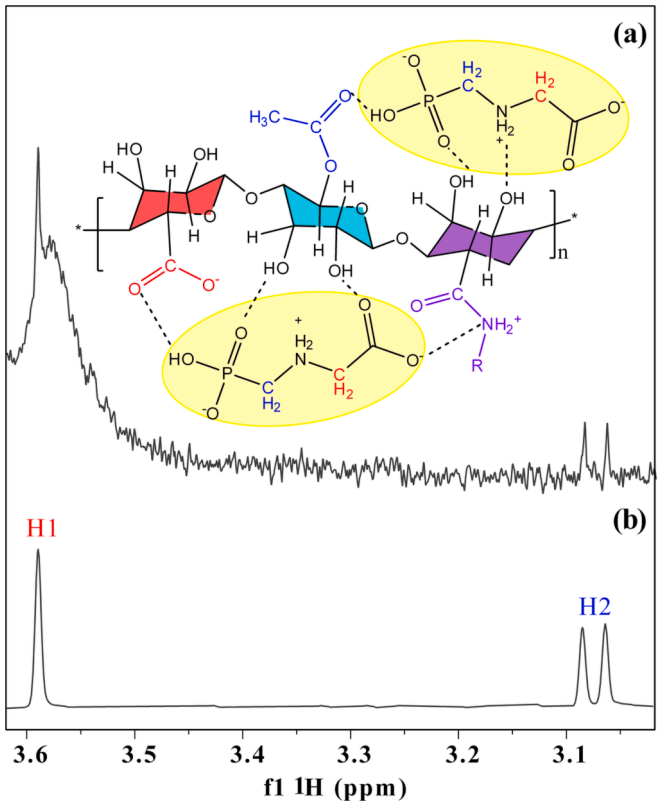

Fig. 1. ^{1}H STD-NMR spectra at pH 5. (a) STD difference spectrum of a sample containing 0.1 mM glyphosate and 20 μM polysaccharide, together with a proposed structure for the PS-glyphosate complex, and (b) reference ^{1}H spectrum of 1 mM glyphosate. Black dashed lines in (a) represent noncovalent bonds. The full-range ^{1}H STD-NMR spectrum of the PS-glyphosate complex is shown in Fig. S4.

correlations were observed for the PS sample, indicating reversible association in bulk solution. In fact, both H1 and H2 protons were visible in STD difference spectra indicating glyphosate attach to hydrophilic moieties of PS chains through noncovalent interactions (Fig. 1-a). As previously suggested, this result provides evidence of a host–guest complex formation between glyphosate and PS, similar to that observed with other natural macromolecules [45,58].

3.2. Polysaccharide and goethite form organo-mineral associations

Interfacial ATR-FTIR spectra (Fig. 2 A-1–2) indicate the progression of PS adsorption through increasing signals of skeletal bands of the pyranose rings (e.g., ν(CC)(CO)$_{ring}$) and α-1,4 glycosidic bonds (e.g., ν_{as}(COC)$_{g}$) from 1200 to 950 cm^{-1} [59–61]. Intense peaks within the 1780 – 1200 cm^{-1} range are also observed and are assigned to diverse band types, including methylester (e.g., ν(C═O)$_{e}$), amide (e.g., amide I and II) and carboxylate (e.g., ν_{as}(COO^{-})) of residual groups in GalA rings [39,49,61–66]. A complete list of peak assignments is shown in SI, Table S1. Kinetic data (Fig. 2B), monitored using the ν(CO)(CC)$_{ring}$ peak height, indicates stable OMAs formed between PS and goethite with only a small fraction of adsorbed PS removed from the surface at the end of the stabilization phase (4.8 – 9.6%). The kinetics of PS coating and stabilization are well described by a PFO model (Fig. 2B, and Table S2). Furthermore, estimated $k_{1,ads}$ and $k_{1,des}$ values indicate PS-goethite formation and stabilization are faster with increasing PS concentration. As shown by identical surface morphology (texture) of SEM images (imaging resolution of ≈ 5 nm), the PS seems to form evenly distributed coatings on synthesized PS-goethite OMAs that result in significant reduction of BET surface area (Fig. 2C - D).

3.3. Glyphosate retention by PS-goethite organo-mineral associations

Batch studies indicate glyphosate adsorption is diminished (52–37%, Table S3) by adsorbed PS (Fig. 3A). The amount of glyphosate retained after desorption is also lower in PS-goethite OMAs compared to goethite (30–13% decrease). However, a reversal to this trend is observed at the highest PS loadings. Zeta potential measurements (Fig. 3B) indicate PS-goethite and glyphosate-PS-goethite complexes developed a negative surface charge whereas goethite (≈ 30 mV) and glyphosate-goethite (≈ 3 mV) are positively charged. Results also indicate the zeta potential of PS-goethite and glyphosate-PS-goethite complexes decreases with increasing PS loading. Decreased adsorption of glyphosate by PS-goethite OMAs relative to goethite can then be explained by electrostatic repulsion between two negatively charged entities. Furthermore, increases in PS surface loading, and corresponding decreases in surface area (Fig. 2C), limits the surface available for adsorption of glyphosate on PS-goethite OMAs. Still, the trend reversal in adsorbed and retained glyphosate corresponds to the extent of PS association on goethite (Fig. 3A). As previously shown in STD difference spectra (Fig. 1-a), the weak attachment of glyphosate to PS may facilitate the retention of glyphosate molecules within adsorbed PS that subsequently leads to this trend reversal. The mechanisms involved in these interactions are

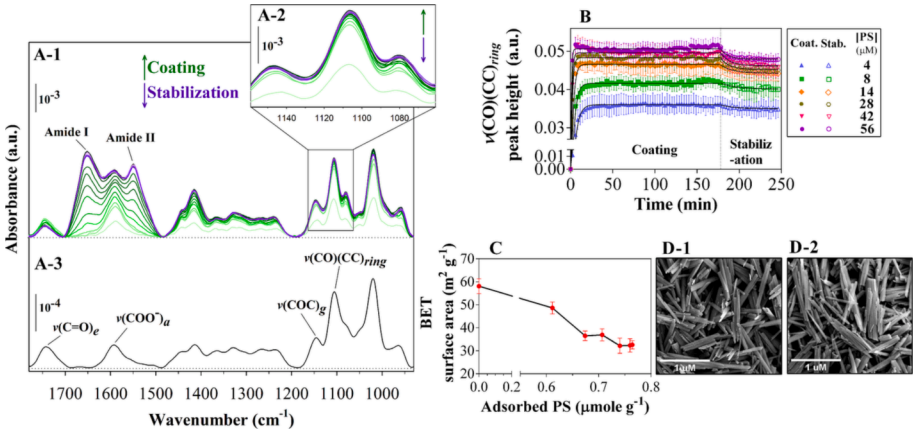

Fig. 2. Formation and stability of PS-goethite OMAs. (A-1) Representative set of *in-situ* ATR-FTIR spectra collected during PS's coating (green lines) and stabilization (purple lines) over a goethite film ([PS] = 8 μM). (A-2) An insert plot of interfacial spectra from 1170 to 1070 cm^{-1}. Spectra collected every ≈ 8 min. (A-3) The solution state spectrum for polysaccharide (112 μM in 10 mM KCl at pH 5.0). (B) Evolution of ν(CO)(CC)$_{ring}$ (1106 cm^{-1}) vibrations during coating and stabilization. (C) BET surface area of PS-goethite OMAs as a function of adsorbed PS. (D) SEM image of (D-1) goethite and (D-2) a PS-goethite OMA (PS ≈ 0.8 μmole g^{-1}).

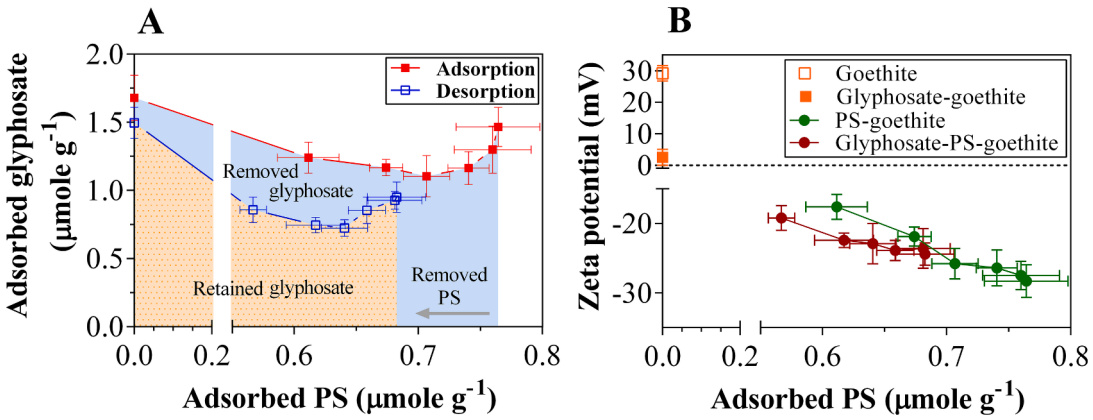

Fig. 3. Results of batch experiments. Influence of adsorbed PS on (A) glyphosate' adsorption and desorption dynamics and (B) zeta potential measurements. Blue and orange areas in A represent the amount of glyphosate removed and retained at equilibrium, respectively. Error bars represent standard deviation values from replicates (n = 3).

discussed in the following sections.

3.4. Contribution of glyphosate' functional groups to interfacial adsorption–desorption and kinetics

Representative *in-situ* time-resolved ATR-FTIR spectra of glyphosate' retention dynamics at the PS-goethite and goethite interface highlight the progression of glyphosate adsorption and desorption through increases and decreases in intensity of the phosphonate, carboxylate, and amine bands of the spectra (Fig. 4A-1 and A-2). In our study, phosphonate ($\nu(PO)$, 1050 – 950 cm^{-1}) and carboxylate-amine ($\nu(CAc)$, 1700 – 1500 cm^{-1}) integrated band areas are considered a measure of glyphosate' surface-associated species [8,12]. Vibrational modes within the $\nu(PO)$ band area include inner-sphere (*IS*) (e.g., P—O—Fe) and outer-sphere (*OS*) (e.g., $(PO_3)_{OS}$ or $(PO_2)_{OS}$) species [8,9,12,14]. The carboxylate-amine $\nu(CAc)$ integrated band area includes surface-associated $\nu_{as}(COO^-)$ and $\delta(NH_2^+)$ vibrational modes [7,8,21].'

Increased PS loading in PS-goethite OMAs impacts glyphosate' adsorption–desorption kinetics and the contribution of observed surface-associated bands (Fig. 4). Consistent with batch experiments, interfacial ATR results show a decrease in intensity of $\nu(PO)$ and $\nu(CAc)$ bands upon glyphosate interaction with PS-goethite OMAs compared to goethite (Fig. 4B – D). These results are in good agreement with Arroyave *et al* [12] where glyphosate adsorption onto humic acid-goethite OMA was hindered, but it is contrary to the results of Guo *et al.* [16] where higher amounts of glyphosate were adsorbed onto humic acid-kaolinite OMA. Variability in the results might be explained by the stability of the OMAs, where humic acid and PS bind strongly onto goethite whereas weak interactions dominate in humic acid-kaolinite OMA.

Adsorption-desorption kinetics for $\nu(PO)$ and $\nu(CAc)$ bands were described by the PSO and PFO kinetic models, respectively (Fig. 4B - C). The estimated PSO and PFO kinetic parameters can be found in SI, Table S4. The $\nu(PO)$- and $\nu(CAc)$-associated adsorption rate constants (k_2

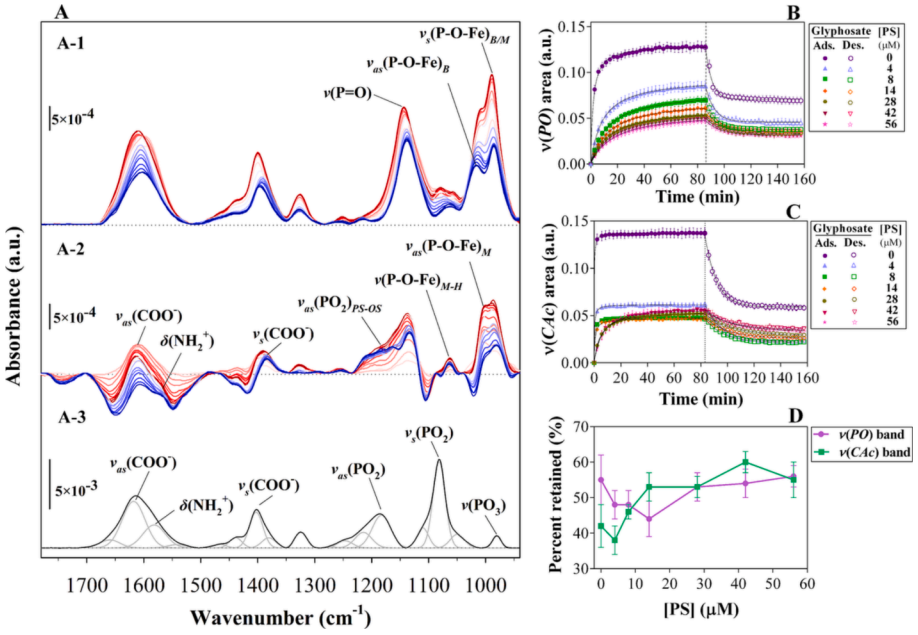

Fig. 4. Representative time-resolved *in-situ* ATR-FTIR spectra collected during glyphosate adsorption and desorption experiments at pH 5 on (A-1) goethite and (A-2) PS-goethite OMAs ([PS] = 14 μM). Red and blue lines indicate the evolution of interfacial spectra collected every ≈ 8 min. (A-3) Solution state ATR-FTIR spectrum of 0.1 M glyphosate in 10 mM KCl at pH 5.0; gray lines show deconvoluted IR components. Evolution of integrated (B) phosphonate ($\nu(PO)$) and (C) carboxylate-amine ($\nu(CAc)$) bands of glyphosate with increased PS surface loading. (D) shows the percentage of $\nu(CAc)$ and $\nu(PO)$ bands retained at the end of the desorption phase (percentage retained = $[A(\tilde{\nu}_i)_{e,des} / A(\tilde{\nu}_i)_{e,ads}] \times 100$]).

$_{(PO),ads}$ and $k_{2,(CAc)ads}$) decreased with increasing PS surface loading on PS-goethite although higher PS loadings had less of an effect on $k_{2(PO),ads}$. These results suggest glyphosate' access to the active sites on goethite was diminished by the primary layer of PS adsorbed at the goethite surface [12]. For the first time, our kinetic modeling shows the carboxylate-amine groups of glyphosate interact with faster kinetics compared to the phosphonate group, particularly at PS surface loadings ≤ 14 μM (Table S4). The fact that different IR bands of the same molecule (i.e., glyphosate) evolve at different rates indicates the presence of more than one interfacial species or it might be caused by interaction with different sites on these heterogeneous surfaces [43,67]. As shown in Fig. 4D, the fraction of $\nu(CAc)$ IR bands retained after desorption increased with increasing PS loading whereas that of $\nu(PO)$ decreased initially but then increased to a value similar to goethite (≥28 μM). This behavior suggests PS-goethite associations may hinder desorption of glyphosate at higher PS loading and is in agreement with retained glyphosate values in batch experiments (Fig. 3A). Still, desorption rate constants ($k_{1,(PO)des}$ and $k_{1,(CAc)des}$) show similar kinetic trends, with the carboxylate-amine groups presenting slower desorption rates at low PS loadings (Table S4). Moreover, adsorbed PS was reduced by 8.5–23.5% upon introduction of glyphosate at the stabilized PS-goethite interface (Fig. S5) whereas no significant changes to the ATR-FTIR spectra of PS-goethite were observed in control experiments after the introduction of 10 mM KCl background solution (Fig. S6). These results suggest glyphosate, and potentially other low molecular weight organics, might have a destabilizing effect on OMAs present in soils [68,69].

The most striking results were found when the $\nu(CAc)$ bands were deconvoluted across all experiments (Fig. S7, Fig. 5) and the contribution of individual IR components calculated. This procedure is fully described in SI, SM7. The carboxylate-amine band ($\nu(CAc)$) of glyphosate (1700 – 1550 cm^{-1}) originates mainly from asymmetrical stretching vibration modes of COO^- and its coupling with deformation modes of the NH_2^+ group [7,8,21,70]. We found glyphosate' $\delta(NH_2^+)$ band contribution to adsorption ($X(\delta(NH_2^+)_{ads}$) increased as a function of PS surface loading, from 28% to 45% (Fig. 5A-1). Conversely, glyphosate $\nu_{as}(COO^-)$ band contribution to adsorption ($X(\nu(COO^-)_{ads}$) diminished with increasing PS surface loading, from 72% to 55%. Although similar trends were observed during the desorption phase (Fig. 5A-2), the remaining surface-associated $X(\delta(NH_2^+)$ increased with increasing PS surface loading ([PS] ≥ 28 μM) to ≈ 60%. The remaining surface-associated $X(\nu(COO^-)_{des}$ diminished to ≈ 40% at PS loadings ≥ 28 μM. Furthermore, Fig. 5B-1 to B-4 and Table S5 indicate surface-associated $\delta(NH_2^+)$ adsorption bands of glyphosate evolved faster than corresponding $\nu_{as}(COO^-)$ bands at higher PS surface loadings (PS ≥ 28 μM). This can be explained by the interfacial electrostatic potential, which is expected to increase for a positive functional group with increasing PS surface loading due to the increased number of carboxylate functionalities available in PS chains (PS used in experiments had an estimated ≈ 37% carboxylate content; see SM1). Interactions between glyphosate-NH_2^+ and O-containing residues in PS chains are therefore deemed favorable through hydrogen bonding and electrostatic interactions [16,61,71,72].

3.5. Mechanisms of interaction

3.5.1. Phosphonate-meditated binding

The predominant species of glyphosate at pH 5.0 and I = 10 mM is the monoanion [$^-$OOCCH$_2$N$^+$H$_2$CH$_2$-HPO$_3^-$] (69.78%), with lesser contributions from its dianion [$^-$OOCCH$_2$N$^+$H$_2$CH$_2$-PO$_3^{2-}$] (30.09%) and trianion [$^-$OOCCH$_2$NHCH$_2$-PO$_3^{2-}$] (0.13%) species (pK_{a2} = 2.3, pK_{a3} = 5.5 and pK_{a4} = 11.0) [19,73,74]. Therefore, glyphosate has the capacity to interact with goethite and PS-goethite interfaces through various functionalities to form surface-associated species of different geometries (Fig. 4A-1 and A-2, and Table S6) [4,7–9,12,14,20,21,75]. The interfacial ATR spectra indicate that Fe—O—P bonds (i.e., *IS* complex) formed

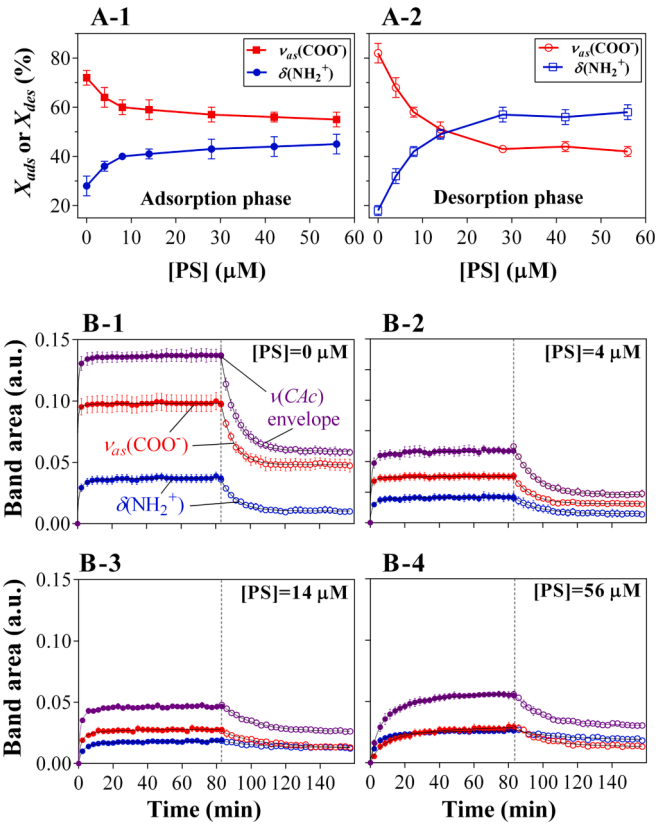

Fig. 5. Contribution (X_{ads} and X_{des}) of deconvoluted $\nu(CAc)$ band components of glyphosate at (A-1) adsorption ($t_{e,ads}$ = 80.0 min) and (A-2) desorption ($t_{e,des}$ = 157.5 min) equilibrium as a function of PS loading. (B) shows the evolution of $\nu(CAc)$ glyphosate band components during adsorption and desorption for (B-1) goethite and (B-2 to B-4) PS-goethite OMAs with increased PS loading. Black lines in B represent PSO and PFO kinetic fits for adsorption and desorption, respectively. Dashed vertical lines split glyphosate' adsorption and desorption phases.

at the goethite interface (1050 – 950 cm^{-1}). It has been suggested that under slightly acidic conditions (e.g., pH = 5) the phosphonate group of glyphosate forms *IS* complexes with goethite, more favorably bidentate (*B*) and monodentate with proton (*M*–*H*), through ligand-exchange reactions [8,9,14]. At pH = 5.0, the electrostatic attraction potential at the goethite surface (pH_{pzc} = 8.4 ± 0.2) increases the energetic favorability to form bidentate complexes through phosphonate groups. Furthermore, our study indicates that an *IS* monodentate complex without proton (*M*) most likely forms due to the contribution of glyphosate' dianion species [8,14]. Besides reducing the number of available surface sites, adsorption of PS diminishes the electrostatic interaction energy between glyphosate' phosphonate group and the goethite surface [76] thus promoting the formation of *IS* monodentate complexes over bidentate. In addition, increase PS loading on PS-goethite OMAs increases the surface negative charge that favors the formation of monodentate complexes [8,9,14]. Since the phosphonate anion is a strong acceptor of hydrogen bonds [77], the downshift for unbonded ν(P═O) (≈ 8 cm^{-1}) in PS-goethite OMAs (Fig. 4A-2, Table S6) is expected to result from intermolecular hydrogen bonds formed between glyphosate' phosphonate group and PS residues in OMAs. Moreover, a new IR feature is observed in ATR-FTIR spectra of PS-goethite OMAs at 1160 – 1164 cm^{-1}. We tentatively assign this new feature to outer-sphere (*OS*) complexes ($\nu_{as}(PO_2)_{PS\text{-}OS}$; i.e., R-PO$_3^-$(H) ··· O/N-PS) which split at lower energies due to hydrogen bonding (Fig. 4A-2). These results are in agreement with high-resolution P 2p XPS spectra (Fig. 6) where increases in binding energy (B.E.) of the P atom 2p envelop upon glyphosate adsorption on goethite (+0.5 eV) and PS-goethite OMAs (+0.5 –

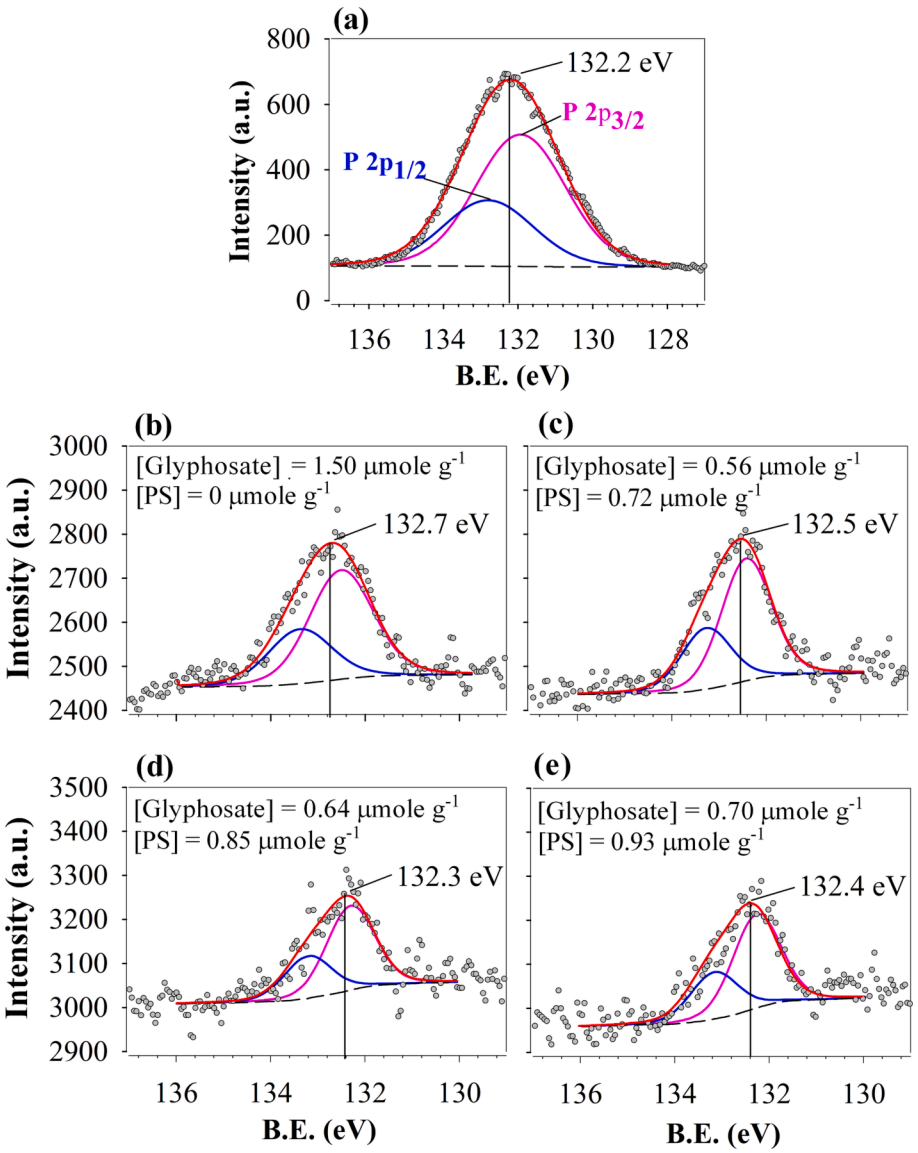

Fig. 6. High resolution P 2p XPS spectra for (a) standard glyphosate salt, (b) glyphosate adsorbed on goethite, and (c – e) glyphosate adsorbed on PS-goethite OMAs. The P 2p spectrum of glyphosate presents two component peaks centered at 131.9 ($2p_{3/2}$) and 132.8 ($2p_{1/2}$) eV, which are associated with the spin–orbit splitting of the P 2p level, with a separation of ≈ 0.9 eV [82]. Solid vertical lines indicate the B.E. of the P 2p XPS spectra envelope.

+0.1 eV) are observed. Increases in B.E. result from decreases in electron density in the P atom of the phosphonate group that occur upon formation of mixed bidentate-monodentate Fe—O—P bonds [78–80]. Greater shifts in P 2p binding energy are associated with bidentate configuration, as is the case for phosphonate group binding on goethite [81].

3.5.2. *Carboxylate and amine-meditated binding*

Changes in peak position of the carboxylate ($\nu_{as}(COO^-)$ and $\nu_s(COO^-)$) and amine ($\delta(NH_2^+)$) vibrational modes of glyphosate are used to decipher carboxylate- and amine-meditated molecular interactions at the goethite and PS-goethite interface [7,8,21,70]. At the goethite interface, both asymmetric and symmetric vibrational modes of the carboxylate group of sorbed glyphosate were subjected to downward shifts (6 – 15 cm^{-1}) (Fig. 4, A-1, and Table S6). Albeit to a lesser extent, downward shifts in $\nu(COO^-)$ were also observed at the PS-goethite interface (Fig. 4, A-2, and Table S6). A reduction in $\nu(COO^-)$ vibrational energy suggest glyphosate' carboxylate group primarily contributes to the formation of *OS* complexes via intermolecular hydrogen bonding that occurs among glyphosate molecules at the goethite surface. These observations are in agreement with previous studies where the adsorption modes of carboxylate-containing organic anions and zwitterions (including glyphosate) on goethite have been investigated [8,9,12,14,21,70,83,84].

As in previous studies [9,14], we found no evidence for the participation of the NH_2^+ group of glyphosate in surface complexation at the goethite interface (Fig. 4, A-1, and Table S6). Interfacial $\delta(NH_2^+)$ vibrational modes of glyphosate however shifted to higher energies (by 7 – 27 cm^{-1}) at the PS-goethite interface (Fig. 4, A-2, and Table S6). These bands also gained intensity relative to interfacial $\nu_{as}(COO^-)$ bands as a function of PS surface loading (Fig. 5 and Table S5). The above-mentioned observations imply glyphosate forms amine-associated hydrogen bonds with PS-goethite OMAs since hydrogen bonds stabilize charged resonance structures [85] and the strength of hydrogen bonds is related to the integrated absorbance of amine bands [72]. Therefore, the corresponding upshifts with increasing PS surface loading denote the involvement of the amine group through stronger hydrogen bonds with carbonyl-containing functional groups of the polysaccharide. Although glyphosate NH_2^+ group is expected to encounter a repulsive force from the mostly positive-charged goethite surface that

establish a barrier for amine-meditated hydrogen bonding, the presence of PS associations may facilitate these interactions due to the development of a negative charge at the surface of PS-goethite OMAs (Fig. 3B).

4. Conclusions

Studies of glyphosate retention dynamics at organo-mineral interfaces, as presented in this work, are environmentally relevant since surface soils contain minerals that are mostly, if not completely, coated with organic molecules. While the fate of glyphosate in soils is strongly influenced by organic-organic interactions (e.g., glyphosate-polysaccharide) that occur within organo-mineral associations (e.g., polysaccharide-goethite), research in this area is still limited and the results inconclusive. Our work contributes to the narrowing of this considerable knowledge gap [8,12,16].

Using model organo-mineral associations (i.e., polysaccharide-goethite OMAs), our experiments indicate the amount of mineral-adsorbed organic matter modulates the extent, kinetics, and mechanisms of interaction of glyphosate under conditions relevant to agricultural soils of humid regions. The extent of glyphosate retention at polysaccharide-goethite interfaces was reduced compared to that at the goethite interface. At the same time, increased polysaccharide surface loading resulted in slower glyphosate adsorption and desorption kinetics compared to corresponding processes at the goethite interface. Mechanistically, increases in PS surface loading resulted in the successive disappearance of glyphosate inner-sphere bidentate configurations on goethite while promoting the formation of inner-sphere monodentate configurations. Furthermore, the adsorbed polysaccharide promoted the formation of outer-sphere surface species through intermolecular hydrogen bonds between the functional groups of glyphosate and functional groups at goethite and polysaccharide-goethite interfaces. Based on the results of this investigation, we suggest studies with bare mineral surfaces [9,44,86–88] are likely to underestimate glyphosate mobility and transport in soils since organo-mineral associations can reduce both the adsorption capacity and kinetics, in addition to promoting the formation of presumably weaker mechanisms of interaction.

The results of these studies highlight the impact organo-mineral associations might have on glyphosate' mobility and retention at heterogeneous interfaces present in soils. But since the proportion of organo-mineral to mineral interfaces is higher in surface soils, our work provides insights as to the extent, kinetics and mechanisms that might be involved during glyphosate downward transport. Ultimately, this knowledge and further molecular-scale studies with a variety of organo-mineral interfaces could lead to better predictions of glyphosate occurrence in natural systems and risk assessments.

Declaration of Competing Interest

The authors declare that they have no known competing financial interests or personal relationships that could have appeared to influence the work reported in this paper.

Data availability

Data will be made available on request.

Acknowledgments and funding

Funding for this work was provided by the National Science Foundation (Award number CHE-2003505) and by the USDA National Institute of Food and Agriculture, Hatch project (accession no. 1020955). Graduate financial support for B.A. was provided by the National Science Foundation (Award number CHE-2003505), by the Agriculture and Food Research Initiative (AFRI, grant no. 2016–67019-25265/project accession no. 1009565) from the USDA National Institute of Food and Agriculture and by the College of Agriculture and Life Sciences at Cornell University. Partial research funding was also provided by a Graduate Research grant from the Schmittau-Novak Small Grant Program from the School of Integrative Plant Science, Cornell University. This work made use of the Cornell Center for Materials Research Shared Facilities supported by the National Science Foundation MRSEC program under Award Number DMR-1719875 and of the NMR facility in the Department of Chemistry and Chemical Biology at Cornell University.

Appendix A. Supplementary data

Supplementary data to this article can be found online at https://doi.org/10.1016/j.jcis.2023.09.141.

References

[1] P. Nadin, The use of plant protection products in the European union data 1992–2003, Luxembourg, France, European Commission, 2007.
[2] H. Li, A.F. Wallace, M. Sun, P. Reardon, D.P. Jaisi, Degradation of glyphosate by Mn-oxide may bypass sarcosine and form glycine directly after C-N bond cleavage, Environ. Sci. Tech. 52 (3) (2018) 1109–1117.
[3] C. Huhn, More and enhanced glyphosate analysis is needed, Anal. Bioanal. Chem. 410 (13) (2018) 3041–3045.
[4] T. Undabeytia, E. Morillo, C. Maqueda, FTIR study of glyphosate−copper complexes, J. Agric. Food Chem. 50 (7) (2002) 1918–1921.
[5] V. Subramaniam, P.E. Hoggard, Metal complexes of glyphosate, J. Agric. Food Chem. 36 (6) (1988) 1326–1329.
[6] J. Sheals, P. Persson, B. Hedman, IR and EXAFS spectroscopic studies of glyphosate protonation and copper(II) complexes of glyphosate in aqueous solution, Inorg. Chem. 40 (17) (2001) 4302–4309.
[7] B.C. Barja, M. dos Santos Afonso, An ATR−FTIR study of glyphosate and its Fe(III) complex in aqueous solution, Environ. Sci. Tech. 32 (21) (1998) 3331–3335.
[8] W. Yan, C. Jing, Molecular insights into glyphosate adsorption to goethite gained from ATR-FTIR, two-dimensional correlation spectroscopy, and DFT study, Environ. Sci. Technol. 52 (4) (2018) 1946–1953.
[9] J. Sheals, S. Sjöberg, P. Persson, Adsorption of glyphosate on goethite: molecular characterization of surface complexes, Environ. Sci. Tech. 36 (14) (2002) 3090–3095.
[10] E.J. Elzinga, D.L. Sparks, Phosphate adsorption onto hematite: An in situ ATR-FTIR investigation of the effects of pH and loading level on the mode of phosphate surface complexation, J. Colloid Interface Sci. 308 (1) (2007) 53–70.
[11] C.N. Albers, G.T. Banta, P.E. Hansen, O.S. Jacobsen, The influence of organic matter on sorption and fate of glyphosate in soil–Comparing different soils and humic substances, Environ. Pollut. 157 (10) (2009) 2865–2870.
[12] J.M. Arroyave, C.C. Waiman, G.P. Zanini, M.J. Avena, Effect of humic acid on the adsorption/desorption behavior of glyphosate on goethite, Isotherms and kinetics, Chemosphere 145 (2016) 34–41.
[13] K.A. Barrett, M.B. McBride, Oxidative degradation of glyphosate and aminomethylphosphonate by manganese oxide, Environ. Sci. Tech. 39 (23) (2005) 9223–9228.
[14] B.C. Barja, M. dos Santos Afonso, Aminomethylphosphonic acid and glyphosate adsorption onto goethite: a comparative study, Environ. Sci. Tech. 39 (2) (2005) 585–592.
[15] R.L. Glass, Adsorption of glyphosate by soils and clay minerals, J. Agric. Food Chem. 35 (4) (1987) 497–500.
[16] F. Guo, M. Zhou, J. Xu, J.B. Fein, Q. Yu, Y. Wang, Q. Huang, X. Rong, Glyphosate adsorption onto kaolinite and kaolinite-humic acid composites: Experimental and molecular dynamics studies, Chemosphere 263 (2021), 127979.
[17] R. Sutton, G. Sposito, Molecular structure in soil humic substances: the new view, Environ. Sci. Tech. 39 (23) (2005) 9009–9015.
[18] M. McBride, K.-H. Kung, Complexation of glyphosate and related ligands with iron (III), Soil Sci. Soc. Am. J. 53 (6) (1989) 1668–1673.
[19] L. Tribe, K.D. Kwon, C.C. Trout, J.D. Kubicki, Molecular orbital theory study on surface complex structures of glyphosate on goethite: calculation of vibrational frequencies, Environ. Sci. Tech. 40 (12) (2006) 3836–3841.
[20] C.V. Waiman, M.J. Avena, A.E. Regazzoni, G.P. Zanini, A real time in situ ATR-FTIR spectroscopic study of glyphosate desorption from goethite as induced by phosphate adsorption: Effect of surface coverage, J. Colloid Interface Sci. 394 (2013) 485–489.
[21] Y. Yang, S. Wang, Y. Xu, B. Zheng, J. Liu, Molecular-scale study of aspartate adsorption on goethite and competition with phosphate, Environ. Sci. Tech. 50 (6) (2016) 2938–2945.
[22] M.P. Schmidt, C.E. Martínez, Supramolecular association impacts biomolecule adsorption onto goethite, Environ. Sci. Tech. 52 (7) (2018) 4079–4089.
[23] D. Saxena, S. Flores, G. Stotzky, Vertical movement in soil of insecticidal Cry1Ab protein from Bacillus thuringiensis, Soil Biol. Biochem. 34 (1) (2002) 111–120.
[24] M.P. Schmidt, C.E. Martínez, Kinetic and conformational insights of protein adsorption onto montmorillonite revealed using in situ ATR-FTIR/2D-COS, Langmuir 32 (31) (2016) 7719–7729.
[25] L.H. de Oliveira, P. Trigueiro, B. Rigaud, E.C. da Silva-Filho, J.A. Osajima, M. G. Fonseca, J.-F. Lambert, T. Georgelin, M. Jaber, When RNA meets

montmorillonite: Influence of the pH and divalent cations, Appl. Clay Sci. 214 (2021), 106234.
[26] M.P. Schmidt, C.E. Martínez, Ironing out genes in the environment: an experimental study of the DNA–goethite interface, Langmuir 33 (34) (2017) 8525–8532.
[27] K.M. Parker, V. Barragán Borrero, D.M. van Leeuwen, M.A. Lever, B. Mateescu, M. Sander, Environmental fate of RNA interference pesticides: adsorption and degradation of double-stranded RNA molecules in agricultural soils, Environ. Sci. Tech. 53 (6) (2019) 3027–3036.
[28] M. Cagnasso, V. Boero, M.A. Franchini, J. Chorover, ATR-FTIR studies of phospholipid vesicle interactions with α-FeOOH and α-Fe2O3 surfaces, Colloids Surf. B Biointerfaces 76 (2) (2010) 456–467.
[29] Q. Liu, Y. Zhang, J.S. Laskowski, The adsorption of polysaccharides onto mineral surfaces: an acid/base interaction, Int. J. Miner. Process. 60 (3) (2000) 229–245.
[30] A. Tétrault, Y. Gélinas, Preferential sorption of polysaccharides on mackinawite: A chemometrics approach, Geochim. Cosmochim. Acta 337 (2022) 61–72.
[31] R. Mikutta, A. Baumgärtner, A. Schippers, L. Haumaier, G. Guggenberger, Extracellular polymeric substances from bacillus subtilis associated with minerals modify the extent and rate of heavy metal sorption, Environ. Sci. Tech. 46 (7) (2012) 3866–3873.
[32] T. Guhra, T. Ritschel, K.U. Totsche, Formation of mineral–mineral and organo–mineral composite building units from microaggregate-forming materials including microbially produced extracellular polymeric substances, Eur. J. Soil Sci. 70 (3) (2019) 604–615.
[33] A. Omoike, J. Chorover, K.D. Kwon, J.D. Kubicki, Adhesion of bacterial exopolymers to α-FeOOH: inner-sphere complexation of phosphodiester groups, Langmuir 20 (25) (2004) 11108–11114.
[34] M. Kleber, K. Eusterhues, M. Keiluweit, C. Mikutta, R. Mikutta, P.S. Nico, Chapter one - mineral-organic associations: formation, properties, and relevance in soil environments, in: D.L. Sparks (Ed.), Advances in Agronomy, Academic Press, 2015, pp. 1–140.
[35] C.J. Newcomb, N.P. Qafoku, J.W. Grate, V.L. Bailey, J.J. De Yoreo, Developing a molecular picture of soil organic matter–mineral interactions by quantifying organo–mineral binding, Nat. Commun. 8 (1) (2017) 396.
[36] I. Kögel-Knabner, The macromolecular organic composition of plant and microbial residues as inputs to soil organic matter, Soil Biol. Biochem. 34 (2) (2002) 139–162.
[37] N. Manucharova, The microbial destruction of chitin, pectin, and cellulose in soils, Eurasian Soil Sci. 42 (13) (2009) 1526–1532.
[38] D. Mohnen, Pectin structure and biosynthesis, Curr. Opin. Plant Biol. 11 (3) (2008) 266–277.
[39] A.K. Chatjigakis, C. Pappas, N. Proxenia, O. Kalantzi, P. Rodis, M. Polissiou, FT-IR spectroscopic determination of the degree of esterification of cell wall pectins from stored peaches and correlation to textural changes, Carbohydr. Polym. 37 (4) (1998) 395–408.
[40] E. De Gerónimo, V.C. Aparicio, Changes in soil pH and addition of inorganic phosphate affect glyphosate adsorption in agricultural soil, Eur. J. Soil Sci. 73 (1) (2022) e13188.
[41] B. Zhao, J. Zhang, J. Gong, H. Zhang, C. Zhang, Glyphosate mobility in soils by phosphate application: Laboratory column experiments, Geoderma 149 (3) (2009) 290–297.
[42] R.C. Pereira, P.R. Anizelli, E. Di Mauro, D.F. Valezi, A.C.S. da Costa, C.T.B.V. Zaia, D.A.M. Zaia, The effect of pH and ionic strength on the adsorption of glyphosate onto ferrihydrite, Geochem. Trans. 20 (1) (2019) 3.
[43] M.P. Schmidt, S.D. Siciliano, D. Peak, Spectroscopic quantification of inner- and outer-sphere oxyanion complexation kinetics: ionic strength and background cation effect on sulfate adsorption to hematite, ACS Earth Space Chem. 4 (10) (2020) 1765–1776.
[44] C.V. Waiman, J.M. Arroyave, H. Chen, W. Tan, M.J. Avena, G.P. Zanini, The simultaneous presence of glyphosate and phosphate at the goethite surface as seen by XPS, ATR-FTIR and competitive adsorption isotherms, Colloids Surf. A Physicochem. Eng. Asp. 498 (2016) 121–127.
[45] P. Mazzei, A. Piccolo, Quantitative evaluation of noncovalent interactions between glyphosate and dissolved humic substances by NMR spectroscopy, Environ. Sci. Tech. 46 (11) (2012) 5939–5946.
[46] C.A. Hettiarachchi, L.D. Melton, M.A. Williams, D.J. McGillivray, J.A. Gerrard, S. M. Loveday, M orphology of complexes formed between β-lactoglobulin nanofibrils and pectins is influenced by the pH and structural characteristics of the pectins, Biopolymers 105 (11) (2016) 819–831.
[47] B.M. Yapo, Rhamnogalacturonan-I: a structurally puzzling and functionally versatile polysaccharide from plant cell walls and mucilages, Polym. Rev. 51 (4) (2011) 391–413.
[48] D.A. Méndez, M.J. Fabra, L. Gómez-Mascaraque, A. López-Rubio, A. Martinez-Abad, Modelling the extraction of pectin towards the valorisation of watermelon rind waste, Foods 10 (4) (2021) 738.
[49] P.L. Rockwell, M.A. Kiechel, J.S. Atchison, L.J. Toth, C.L. Schauer, Various-sourced pectin and polyethylene oxide electrospun fibers, Carbohydr. Polym. 107 (2014) 110–118.
[50] U. Schwertmann, R.M. Cornell, Iron oxides in the laboratory: preparation and characterization, John Wiley & Sons, 2008.
[51] A. Viegas, J. Manso, F.L. Nobrega, E.J. Cabrita, Saturation-transfer difference (STD) NMR: a simple and fast method for ligand screening and characterization of protein binding, J. Chem. Educ. 88 (7) (2011) 990–994.
[52] T.C. Catrinck, A. Dias, M.C.S. Aguiar, F.O. Silvério, P.H. Fidêncio, G.P. Pinho, A simple and efficient method for derivatization of glyphosate and AMPA using 9-fluorenylmethyl chloroformate and spectrophotometric analysis, J. Braz. Chem. Soc. 25 (2014) 1194–1199.
[53] D.E. Felton, M. Ederer, T. Steffens, P.L. Hartzell, K.V. Waynant, UV–vis spectrophotometric analysis and quantification of glyphosate for an interdisciplinary undergraduate laboratory, J. Chem. Educ. 95 (1) (2018) 136–140.
[54] Y.-S. Ho, Review of second-order models for adsorption systems, J. Hazard. Mater. 136 (3) (2006) 681–689.
[55] W. Plazinski, W. Rudzinski, A. Plazinska, Theoretical models of sorption kinetics including a surface reaction mechanism: A review, Adv. Colloid Interface Sci. 152 (1) (2009) 2–13.
[56] S. Lagergren, Zur theorie der sogenannten adsorption geloster stoffe, Kungliga svenska vetenskapsakademiens. Handlingar 24 (1898) 1–39.
[57] B. Cartigny, N. Azaroual, M. Imbenotte, D. Mathieu, G. Vermeersch, J.P. Goullé, M. Lhermitte, Determination of glyphosate in biological fluids by 1H and 31P NMR spectroscopy, Forensic Sci. Int. 143 (2) (2004) 141–145.
[58] K. Ariga, T. Kunitake, Supramolecular chemistry-fundamentals and applications: advanced textbook, Springer Science & Business Media, 2006.
[59] A. Synytsya, J. Čopíková, P. Matějka, V. Machovič,, Fourier transform Raman and infrared spectroscopy of pectins, Carbohydr. Polym. 54 (1) (2003) 97–106.
[60] I. Šimkovic, A. Synytsya, I. Uhliariková, J. Čopíková, Amidated pectin derivatives with n-propyl-, 3-aminopropyl-, 3-propanol- or 7-aminoheptyl-substituents, Carbohydr. Polym. 76 (4) (2009) 602–606.
[61] A. Sinitsya, J. Čopíková, V. Prutyanov, S. Skoblya, V. Machovič, Amidation of highly methoxylated citrus pectin with primary amines, Carbohydr. Polym. 42 (4) (2000) 359–368.
[62] F. Meneguzzo, C. Brunetti, A. Fidalgo, R. Ciriminna, R. Delisi, L. Albanese, F. Zabini, A. Gori, L.B. dos Santos Nascimento, A. De Carlo, F. Ferrini, L.M. Ilharco, M. Pagliaro, Real-scale integral valorization of waste orange peel via hydrodynamic cavitation, Processes 7 (9) (2019) 581.
[63] A. Fidalgo, R. Ciriminna, D. Carnaroglio, A. Tamburino, G. Cravotto, G. Grillo, L. M. Ilharco, M. Pagliaro, Eco-friendly extraction of pectin and essential oils from orange and lemon peels, ACS Sustain. Chem. Eng. 4 (4) (2016) 2243–2251.
[64] A. Assifaoui, C. Loupiac, O. Chambin, P. Cayot, Structure of calcium and zinc pectinate films investigated by FTIR spectroscopy, Carbohydr. Res. 345 (7) (2010) 929–933.
[65] M.H.G. Canteri, C.M.G.C. Renard, C. Le Bourvellec, S. Bureau, ATR-FTIR spectroscopy to determine cell wall composition: Application on a large diversity of fruits and vegetables, Carbohydr. Polym. 212 (2019) 186–196.
[66] S. Guzman-Puyol, J.J. Benítez, E. Domínguez, I.S. Bayer, R. Cingolani, A. Athanassiou, A. Heredia, J.A. Heredia-Guerrero, Pectin-lipid self-assembly: influence on the formation of polyhydroxy fatty acids nanoparticles, PLoS One 10 (4) (2015) e0124639.
[67] A.G. Young, A.J. McQuillan, Adsorption/desorption kinetics from ATR-IR spectroscopy. Aqueous oxalic acid on anatase TiO2, Langmuir 25 (6) (2009) 3538–3548.
[68] M. Keiluweit, J.J. Bougoure, P.S. Nico, J. Pett-Ridge, P.K. Weber, M. Kleber, Mineral protection of soil carbon counteracted by root exudates, Nat. Clim. Chang. 5 (6) (2015) 588–595.
[69] Y. Yuan, Z. Zhang, L. Chen, Z. Yang, J. Liu, Facilitated destabilization of physicochemically protected soil organic matter by root-derived low-molecular-weight organic acids, J. Soil. Sediment. 22 (6) (2022) 1677–1686.
[70] K. Norén, J.S. Loring, P. Persson, Adsorption of alpha amino acids at the water/goethite interface, J. Colloid Interface Sci. 319 (2) (2008) 416–428.
[71] Z. Gu, R. Zambrano, A. McDermott, Hydrogen bonding of carboxyl groups in solid-state amino acids and peptides: comparison of carbon chemical shielding, infrared frequencies, and structures, J. Am. Chem. Soc. 116 (14) (1994) 6368–6372.
[72] F.C. Wang, M. Feve, T.M. Lam, J.-P. Pascault, FTIR analysis of hydrogen bonding in amorphous linear aromatic polyurethanes. I. Influence of temperature, J. Polym. Sci. B 32 (8) (1994) 1305–1313.
[73] W. Li, Y.-J. Wang, M. Zhu, T.-T. Fan, D.-M. Zhou, B.L. Phillips, D.L. Sparks, Inhibition mechanisms of Zn precipitation on aluminum oxide by glyphosate: a 31P NMR and Zn EXAFS study, Environ. Sci. Tech. 47 (9) (2013) 4211–4219.
[74] Z. Chen, W. He, M. Beer, M. Megharaj, R. Naidu, Speciation of glyphosate, phosphate and aminomethylphosphonic acid in soil extracts by ion chromatography with inductively coupled plasma mass spectrometry with an octopole reaction system, Talanta 78 (3) (2009) 852–856.
[75] M.C. Zenobi, C.V. Luengo, M.J. Avena, E.H. Rueda, An ATR-FTIR study of different phosphonic acids in aqueous solution, Spectrochim. Acta A Mol. Biomol. Spectrosc. 70 (2) (2008) 270–276.
[76] H.-X. Zhou, X. Pang, Electrostatic interactions in protein structure, folding, binding, and condensation, Chem. Rev. 118 (4) (2018) 1691–1741.
[77] W. Pohle, M. Bohl, H. Böhlig, Interpretation of the influence of hydrogen bonding on the stretching vibrations of the PO−2 moiety, J. Mol. Struct. 242 (1991) 333–342.
[78] L. Zhang, Y. Liu, Y. Wang, X. Li, Y. Wang, Investigation of phosphate removal mechanisms by a lanthanum hydroxide adsorbent using p-XRD, FTIR and XPS, Appl. Surf. Sci. 557 (2021), 149838.
[79] Y. Guo, J. Yu, X. Li, L. Guo, C. Xiao, R. Chi, H. Hou, G. Feng, Selective recovery of glyphosine from glyphosate mother liquor using a modified biosorbent: Competitive substitution adsorption, Environ. Res. 215 (2022), 114394.
[80] M. Mallet, K. Barthélémy, C. Ruby, A. Renard, S. Naille, Investigation of phosphate adsorption onto ferrihydrite by X-ray photoelectron spectroscopy, J. Colloid Interface Sci. 407 (2013) 95–101.
[81] M. Wagstaffe, A.G. Thomas, M.J. Jackman, M. Torres-Molina, K.L. Syres, K. Handrup, An experimental investigation of the adsorption of a phosphonic acid on the anatase TiO2 (101) surface, J. Phys. Chem. C 120 (3) (2016) 1693–1700.

[82] B.D. Ratner, D.G. Castner, Electron spectroscopy for chemical analysis, Surf. Analysis: the Principal Techniques 2 (2009) 374–381.
[83] J. Liang, J.H. Horton, Interactions of benzoic acid and phosphates with iron oxide colloids using chemical force titration, Langmuir 21 (23) (2005) 10608–10614.
[84] K. Norén, P. Persson, Adsorption of monocarboxylates at the water/goethite interface: The importance of hydrogen bonding, Geochim. Cosmochim. Acta 71 (23) (2007) 5717–5730.
[85] N.S. Myshakina, Z. Ahmed, S.A. Asher, Dependence of amide vibrations on hydrogen bonding, J. Phys. Chem. B 112 (38) (2008) 11873–11877.
[86] G.A. Khoury, T.C. Gehris, L. Tribe, R.M.T. Sánchez, M. dos Santos Afonso, Glyphosate adsorption on montmorillonite: An experimental and theoretical study of surface complexes, Appl. Clay Sci. 50 (2) (2010) 167–175.
[87] A.A. Ahmed, P. Leinweber, O. Kühn, Unravelling the nature of glyphosate binding to goethite surfaces by ab initio molecular dynamics simulations, PCCP 20 (3) (2018) 1531–1539.
[88] E. Morillo, T. Undabeytia, C. Maqueda, Adsorption of glyphosate on the clay mineral montmorillonite: effect of Cu (II) in solution and adsorbed on the mineral, Environ. Sci. Tech. 31 (12) (1997) 3588–3592.